8th International Congress of Croatian Society of Mechanics
29 September – 2 October 2015
Opatija, Croatia

Analysis and Simulation of Stewart Platform Manipulator Behavior Driven by Pneumatic Cylinders Applied in Wood Processing

Novak NEDIĆ, Ljubomir LUKIĆ, Dragan PRŠIĆ,

Vladimir STOJANOVIĆ, Duško DUBONJIĆ*

*University of Kragujevac, Faculty of Mechanical and Civil Engineering in Kraljevo
Dositejeva 19, 36000 Kraljevo, Serbia
E-mails: {nedic.n, lukic.lj, prsic.d, stojanovic.v}@mfkv.kg.ac.rs, duka4cz@gmail.com

Abstract. Modern development of machine tools includes investigation of advantages of machines based on a parallel kinematic structure with multiple degrees of freedom. Hence, Stewart platform based on a parallel kinematic structure with six degrees of freedom, achieved with six cylinders pivotally connected to the lower fixed plate and the upper moving plate, is gaining in importance. The advantage of this structure is greater stiffness and accuracy, smaller drives, etc., but smaller workspace. The wood processing industry increasingly requires performing complex spatial forms with high accuracy whose forming occurs at high speeds. Since environmental, energy and maintenance requirements become stricter, the pneumatically driven Stewart platform becomes more and more interesting. The problem of air compressibility and achieving complex trajectory of high static and dynamic accuracy as well as repeatability with high speeds becomes an important factor in understanding the development and selection of robotic platforms. These requirements unavoidably look for understanding kinematics and dynamics of new machines including their drives, and then control algorithms. The paper focuses on analysis and simulation of the behavior of these machines, i.e. realization of the exact position of the moving plate as a base for high quality woodworking. Particularly for processing large and complex products. The analysis is based on the formulation of Lagrange equations of the second type, determining the Jacobian matrix for mechanical part and forming models for the pneumatic actuator (cylinder + valve). The simulation is performed using the MATLAB/Simulink software. Input signals of valves are formed on the basis of desired position of the plate for the chosen platform and drives. The machine is characterized by a larger working space, i.e. longer working strokes of pneumatic cylinders. Hence, it will be considered the impact of the complexity of the desired trajectory platforms, stroke lengths, speed, compressibility etc., on the accuracy of achieving the position of the platform.

1 Introduction

Development of machines based on platforms with parallel mechanism is essential in the development of the wood industry. Industrial robot is a reprogrammable multifunctional manipulator designed to move and process material (wood), through various programmed movements, in order to perform desired tasks. The main disadvantages can be overcome by using parallel manipulators, enabling the most

serious shift and developments in the field of machines based on the application of Stewart's platform.

Besides greater stiffness and accuracy, these robot platforms have high payload-weight ratio due to parallel linkage. Parallel linkage enables the payload distribution and averaging of the positioning error. The payload and positioning errors would be accumulated without parallel linkage.

A pneumatically driven parallel robot platform is obtained through a generalization of the mechanism proposed by Stewart [1] as a flight simulator. As shown in Figure 1, this spatial platform mechanism consists of a fixed base platform and an upper moving platform. The six extendable legs connect these platforms. Accordingly, these types of parallel robot platforms are attractive for certain applications, such as flight simulators, machine tools and force–torque sensors.

Figure1: A 3D model of a 6-DOF parallel robot platform

The pneumatically driven Stewart platform becomes more and more interesting, since environmental, energy and maintenance requirements become stricter [2]. The wood processing industry increasingly requires performing complex reference trajectories with high accuracy of achieving positions the upper moving platform whose realization occurs at high speeds [3]. The problem of air compressibility and achieving complex trajectory of high static and dynamic accuracy as well as repeatability with high speeds becomes an important factor in understanding the development and selection of robotic platforms. These requirements unavoidably look for understanding kinematics and dynamics of new machines including their drives, and then control algorithms [4-7]. The paper focuses on analysis and simulation of the behavior of pneumatically driven Stewart platform, i.e. realization of the exact position of the moving plate as a base for high quality woodworking, particularly for processing large and complex products. The analysis is based on formulation of Lagrange equations of the second type, determining the Jacobian matrix for mechanical part and forming models for the pneumatic actuator (cylinder + valve).

The machine is characterized by a larger working space, i.e. longer working strokes of pneumatic cylinders. MATLAB model is devised to facilitate the analysis and simulation of Stewart platform manipulator behavior driven by pneumatic cylinders applied in wood processing. Furthermore, it will be considered the influence of the complexity of the desired trajectories, stroke lengths, speed, compressibility etc., on the accuracy of achieving the position of the platform.

2 Kinematic model of Stewart platform manipulator

Control of the parallel manipulator (Stewart platform with 6 DOF) is regulated by changing the allowable length of the cylinders that are associated with spherical joint for the upper platform, whose position in the work area depends on the set desired changes in length of the cylinder [4,5], see Figure 2. This relationship determines the change in kinematic properties of Steward's platform. Speed of active joints (actuators) or speed changes of position of the movable platform can be represented by Jacobian matrix.

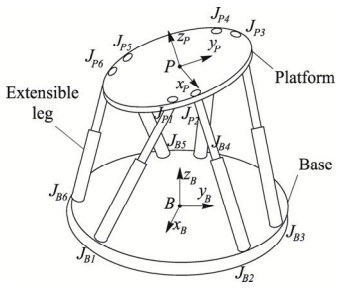

Figure2: Schematic diagram of a 6-DOF parallel robot platform

$$i_i = \left[\vec{w}_i^T \left(\vec{a}_i^T \, x \, \vec{w}_i^T\right)\right] \begin{bmatrix} \vec{v} \\ \vec{\omega} \end{bmatrix} \; i = 1,...,6 \tag{1}$$

where are:
$\vec{a}$ - vector connecting the center of the moving platforms and joint cylinder,
$\vec{w}$ - cylinder unit vector,
$\vec{v}$ - vector which represents a linear speed of moving the upper platform,
$\vec{\omega}$ - vector that represents the angular velocity of moving the upper platform.

This expression can be written for all six cylinders in vector form:

$$i_i = \begin{bmatrix} \vec{w}_1^T & \left(\vec{a}_1^T \, x \, \vec{w}_1^T\right) \\ . & . \\ . & . \\ \vec{w}_6^T & \left(\vec{a}_6^T \, x \, \vec{w}_6^T\right) \end{bmatrix} \begin{bmatrix} \vec{v} \\ \vec{\omega} \end{bmatrix} \tag{2}$$

The matrix that connects the velocity vector changes the length of the legs with the angular and linear speed bogies is Jacobian matrix that depends on the point where the platform is located [3].

$$\vec{i} = J \, \vec{X} \tag{1}$$

3 Dynamic model of Stewart platform manipulator

The dynamic analysis [3] in this paper is solved with the use of Lagrange formulation in order to derive the dynamic equations of the Stewart's manipulator, the whole system is separated into two parts: the moving platform and the legs [4, 5].

3.1 Kinetic and potential energies of the moving platform

The kinetic energy of the moving platform is a summation of two motion energies, since the moving platform has translation and rotation about three orthogonal axes, (*X,Y,Z*) [4, 5].

The first one is translation energy occurring because the translation motion of the center of mass of the moving platform:

$$K_{up(trans)} = \frac{1}{2} m_{up} \left(P_X^2 + P_Y^2 + P_Z^2 \right) \tag{4}$$

where are: m_{up} - is the moving platform mass; $P_{(X,Y,Z)}$ - vector position of the moving platform.

For rotational motion of the moving platform around its center of mass:

$$K_{up(rot)} = \frac{1}{2} \vec{\Omega}_{up(mf)}^T I_{(mf)} \vec{\Omega}_{up(mf)}^T \tag{5}$$

where $I_{(mf)}$ and $\vec{\Omega}_{up(mf)}$ are the rotational inertia mass and the angular velocity of the moving platform, respectively.

Total kinetic energy of the moving platform is:

$$K_{up} = K_{up(trans)} + K_{up(rot)} = \frac{1}{2} m_{up} \left(P_X^2 + P_Y^2 + P_Z^2 \right) + \frac{1}{2} \vec{\Omega}_{up(mf)}^T I_{(mf)} \vec{\Omega}_{up(mf)}^T \tag{6}$$

Potential energy of the moving platform is:

$$P_{up} = m_{up} g P_Z X_{p-o} \tag{7}$$

where $X_{p-0} = \begin{bmatrix} P_x & P_y & P_z & \alpha & \beta & \gamma \end{bmatrix}^T$ represents vector of position and orientation of the moving platform.

3.2 Kinetic and potential energies of the legs

Each leg consists of two parts: the moving part and the fixed part. The kinetic energy [4,5] caused by the rotation around the fixed point B_i:

$$K_{Li} = K_{Li(rot)} + K_{Li(trans)} = \frac{1}{2} (m_1 + m_2) \left[\vec{V}_{Tj}^T h_i \vec{V}_{Tj}^T - L_i k_i L_i \right] \tag{8}$$

where

$$k_i = \frac{\hat{\mathrm{I}}}{L_i} \left(\frac{\hat{\mathrm{I}}}{L_i} + \frac{m_2}{m_1 + m_2} \right) = h_1 - \left(\frac{m_2}{m_1 + m_2} \right)^2 ; \; h_1 = \left(\frac{\hat{\mathrm{I}}}{L_i} + \frac{m_2}{m_1 + m_2} \right)^2 ;$$

$$\hat{\mathrm{I}} = \frac{1}{m_1 + m_2} \left(\delta m_1 l_1 - \frac{1}{2} m_2 l_2 \right);$$

$\vec{V}_{Tj}^{T}$ - is the velocity of the platform connection point of the leg; L_i - the velocity of the active joint; δ - is the distance between B_i and G_i; B_i - is attachment point on the base platform. The kinetic energy of the six legs [3] is:

$$K_{legs} = \sum_{i=1}^{6} K_{Li} = \frac{1}{2} \dot{\mathrm{X}}_{P-0}^{T} \cdot \mathrm{M}_{Legs}\left(\mathrm{X}_{P-0}\right) \cdot \dot{\mathrm{X}}_{P-0} \tag{2}$$

Total potential energy of the legs is:

$$P_{legs} = (m_1 + m_2) g \sum_{i=1}^{3} \left[\hat{\mathrm{I}}\left(\frac{1}{L_{2i}} + \frac{1}{L_{2i}}\right) + \frac{2m_2}{m_1 + m_2} \right] \left(P_Z + Z_{Tj}\right) \tag{3}$$

where is: $Z_{Tj} = \begin{bmatrix} 0 & 0 & 1 \end{bmatrix} R_{Z(\gamma)}^{T} R_{X(\alpha)}^{T} R_{Y(\beta)}^{T} G T_j$

3.3 Dynamic equations

Considering q and τ as the corresponding generalized coordinates and generalized forces, respectively, the general classical equations of the motion can be obtained from the Lagrange formulation [4, 5]:

$$\frac{d}{dt}\frac{dL}{dq} - \frac{\partial L}{\partial q} = \frac{d}{dt}\left(\frac{\partial K(q,\dot{q})}{\partial q}\right) - \frac{\partial K(q,\dot{q})}{\partial q} + \frac{\partial P(q)}{\partial q} = \tau \tag{11}$$

where $K(q,\dot{q})$ is the kinetic energy, and $P(q)$ is the potential energy. Generalized coordinates q is replaced with Cartesian coordinates (X_{p-0}).

4 A dynamic model of pneumatic actuators

For drive upper platform, a pneumatic system composed of the six cylinders controlled by proportional valve are used [8]. Schematic view of double acting, asymmetric pneumatic cylinder with connected four-way spool valve is shown in Figure 3. The external load consists of the mass of external mechanical elements connected to the piston and a force produced by an environmental interaction.

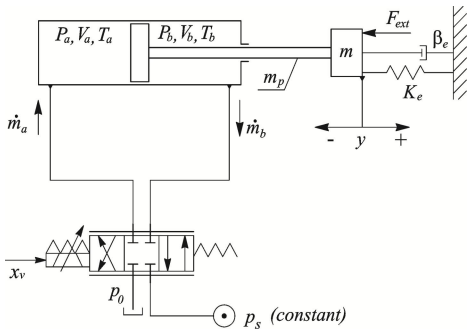

Figure3: Schematic presentation of the valve-controlled asymmetric piston

The present model was established considering the following assumptions:

- The air flow media is a perfect gas,
- The air chamber's thermodynamic states (pressure, temperature and density) within the system components are homogenous,
- The motion of the (piston+rod+load) may be assembly conducted under friction,
- Gas in the chamber and in the pipe are isothermal processes,
- Flow in the servo valve and is isentropic with negligible temperature variation.

An analysis of the dynamic behaviour of a pneumatic system usually requires individual mathematical descriptions of the dynamics of the three component parts of the system: the valve, the actuator and the load. Such analysis is presented below.

4.1 Load dynamics

Applying Newton's second law to the forces on the piston, the resulting force equation is

$$A_a p_a - A_b p_b = m\ddot{y} + \beta_e \dot{y} + F_f(\dot{y}) + K_e y + F_{ext} \tag{12}$$

where p_a and p_b denote the forward and return pressure, respectively, K_e denotes the load spring gradient, β_e is the nonlinear viscous friction coefficient, and F_{ext} denotes the load force disturbance on the piston. The piston displacement y depends on the action of fluid pressures as well as on the load referred to the piston. This load can be seen as summing effects of inertia which comes from the total piston mass m_t, friction forces F_f, spring load forces $K_e y$ and disturbance forces F_{ext}. The total mass of the piston m_t in addition to the mass of piston rod m_p also includes the mass m of the load referred to the piston. The term F_f in equation (12) describes the summing nonlinear effects of static and Coulomb friction forces of the system. Further analysis and description of friction forces can be found in [9]. The area ratio of the asymmetric piston is $A_a / A_b > 1$, where A_a is the effective area of the head side of the piston, and A_b is the effective area of the rod side of the piston, see Figure 3.

4.2 Flow relationships for the control valves

According to assumptions, the flow in the valve is modeled as follows [8]:

$$\dot{m}_i(P_i, P_s, P_0) = C_d W_s f(P_i, P_s, P_0) x_s \tag{4}$$

where $i = a, b$. These subscripts denote inlet and outlet chambers, respectively. For the convenience of the analysis, the following functions are introduced:

$$f(P_a,P_s,P_0)=\begin{cases}\dfrac{P_s\overline{f}\left(\dfrac{P_a}{P_s}\right)}{\sqrt{RT_s}} & if\ x_s\geq 0\\ \dfrac{P_a\overline{f}\left(\dfrac{P_0}{P_a}\right)}{\sqrt{RT_a}} & if\ x_s<0\end{cases},\qquad f(P_b,P_s,P_0)=\begin{cases}\dfrac{P_b\overline{f}\left(\dfrac{P_0}{P_b}\right)}{\sqrt{RT_b}} & if\ x_s\geq 0\\ \dfrac{P_s\overline{f}\left(\dfrac{P_b}{P_s}\right)}{\sqrt{RT_s}} & if\ x_s<0\end{cases} \tag{5}$$

where C_d is the orifice discharge coefficient, W_s is the geometric orifice area of the servo valve, P_s and T_s are respectively the pressure and the temperature of the air supply, P_0 and T_0 are respectively the pressure and the temperature of the atmosphere. To take into account of subsonic and sonic flow, the piecewise flow function $\overline{f}$ is defined as follows:

$$\overline{f}(y)=\begin{cases}\sqrt{\dfrac{2\gamma}{\gamma-1}}\sqrt{y^{\frac{2}{\gamma}}-y^{\frac{\gamma+1}{\gamma}}} & if\ y\geq r_c\\ \sqrt{\gamma\left(\dfrac{2}{\gamma+1}\right)^{\frac{\gamma+1}{\gamma-1}}} & if\ y<r_c\end{cases} \tag{6}$$

The critical pressure ratio r_c is given by:

$$r_c=\left(\frac{2}{\gamma+1}\right)^{\frac{\gamma}{\gamma-1}} \tag{7}$$

in which γ denotes the ratio of specific heats of gaseous medium.

4.3 Dynamic relationship within the control chambers

A model for the mass flow into each of the cylinder chambers can be obtained from the energy conservation equation for the control volume bounded by the cylinder and piston [8]. The control volume energy is given by $c_V\rho VT_s$, where V is the cylinder volume, T_s is the cylinder air temperature, ρ is the air density, and c_V is the specific heat of air at constant volume. If the air flows into the cylinder is assumed to be an adiabatic process of a perfect gas, the change in energy due to the mass transport equals

$$\frac{d}{dt}\left(c_v\rho VT_S\right)=\dot{m}c_pT_S-P\dot{V} \tag{17}$$

where c_p is the specific heat of air at a constant pressure. Assuming an ideal gas, $P=R\rho T$ where R is the universal gas constant. Bearing this in mind, from (17) one can obtain:

$$\dot{m}=\frac{P}{c_pT_S}\dot{V}+\frac{1}{kRT_S}\frac{d(PV)}{dt} \tag{18}$$

in which $k = \frac{c_P}{c_V}$ is the ratio of specific heats for air at the temperature T_s. For a ideal gas, it holds:

$$\frac{1}{R} = \frac{1}{c_p} + \frac{1}{kR} \tag{19}$$

so the mass flow for cylinder chambers can be written in the following form:

$$\dot{m}_i = \frac{1}{RT_S}\left(P_i\dot{V}_i + \frac{V_i}{k}\dot{P}_i\right) \tag{20}$$

where $i = a,b$. Finally, from equations (13)-(16) and (20), the following equations can be derived:

$$\dot{P}_a = -\frac{k\dot{V}_a}{V_a}P_a + \frac{k}{V_a}RT_S C_d W_S f\left(P_a, P_S, P_0\right)x_S \tag{21}$$

$$\dot{P}_b = -\frac{k\dot{V}_b}{V_b}P_b + \frac{k}{V_b}RT_S C_d W_S f\left(P_b, P_S, P_0\right)x_S \tag{22}$$

The total fluid volumes of two cylinder sides, V_a and V_b, are given as:

$$V_a = V_{a0} + yA_a \text{ and } V_b = V_{b0} + \left(L - y\right)A_a \tag{23}$$

where L is the piston stroke and V_{a0} and V_{b0} represent initial chamber volumes. Equations (12), (21) and (22) completely define the nonlinear model of the valve-controlled pneumatic cylinder.

5 Analysis and Simulation results

The analysis is performed using the MATLAB/Simulink software. Input signals of valves are formed on the basis of desired position of the plate for the chosen platform and drives. The system parameters are selected based upon their actual values: areas of the head and rod side of the piston $A_1 = 5\cdot10^{-3}m^2$ and $A_2 = 2.3\cdot10^{-3}m^2$, respectively, supply pressure $p_s = 2.5MPa$, mass of the upper platform $m_p = 50kg$, mass of the piston $m_{pi} = 2kg$, mass of the cylinder $m_{Ci} = 15kg$, radius of the base platform $R_B = 0.8m$, radius of the upper platform $R_P = 0.4m$.

The impact of the complexity of the desired trajectory platforms, stroke lengths, and speed on the accuracy of achieving positions of the pneumatically driven extensible actuators and the position of the platform will be considered. Firstly, let us consider the case when piston strokes are $L = 0.4\ m$ moving upper platform along the y-

axis: $y_{ref} = 0.4\sin(2\pi t)\,[m]$. The accuracy of achieving the positions of six legs and upper moving platform, are shown in Figures 4-5.

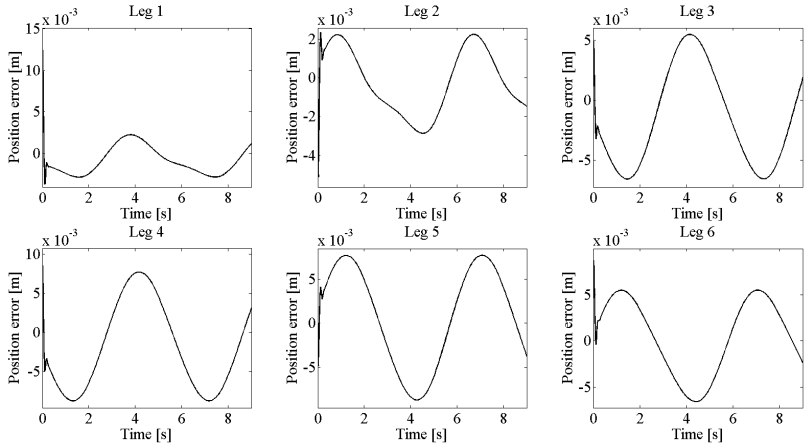

Figure4: The accuracy of achieving the positions of the pneumatically driven extensible actuators moving along the y-axis

Now, consider the complex reference trajectory:

$$x_{ref} = 0.4\sin(2\pi t)[m],\ y_{ref} = 0.4\sin(2\pi t + \pi/2)[m],\ z_{ref} = 0.5 + 0.4\sin(2\pi t)[m] \quad (24)$$

In this case, the accuracy of achieving the positions of six legs and upper moving platform, are shown in Figures 6-7.

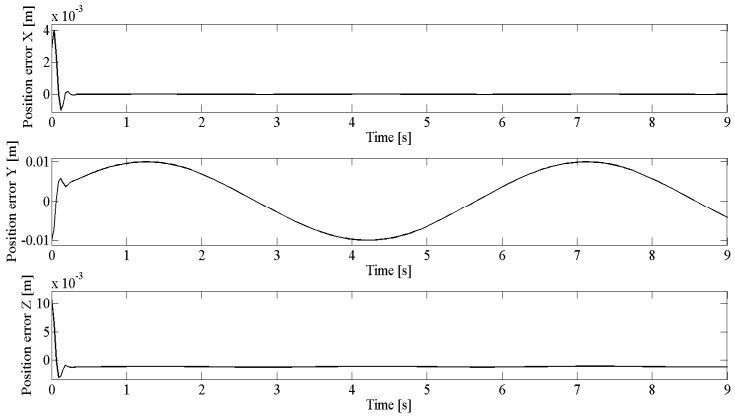

Figure5: The accuracy of achieving the position of the upper platform moving along the y-axis

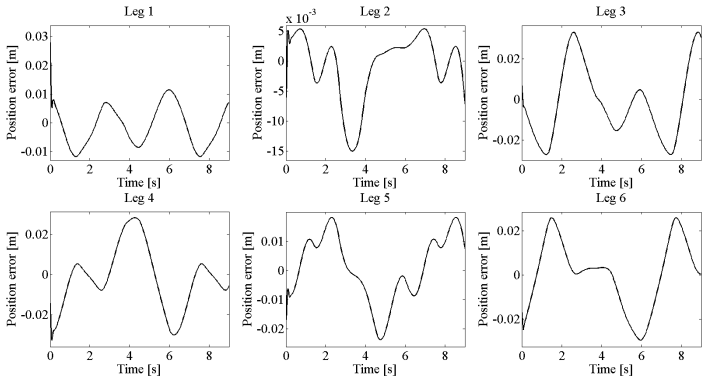

Figure6: The accuracy of achieving the positions of the pneumatically driven extensible actuators

By comparing Figures 4-5 and Figures 6-7 one can conclude that with the increasing complexity of realized trajectories, the accuracy is reduced. Further, let us consider the case when the complex reference trajectory has frequency 2[Hz]:

$$x_{ref} = 0.4\sin(4\pi t)[m],\ y_{ref} = 0.4\sin(4\pi t + \pi/2)[m],\ z_{ref} = 0.5 + 0.4\sin(4\pi t)[m] \quad (25)$$

In this case, the accuracy of achieving the positions of six legs and upper moving platform, are shown in Figures 8-9.

By comparing Figures 6-7 with Figures 8-9 one can conclude that at a higher frequency it is achieved less accuracy of achieving the positions.

Finally, consider now the impact of piston strokes on the accuracy of achieving positions. The piston stroke is $L = 0.8[m]$ and reference trajectory has frequency 2[Hz]. The accuracy of achieving the positions of six legs and upper moving platform in this case, are shown in Figures 10-11.

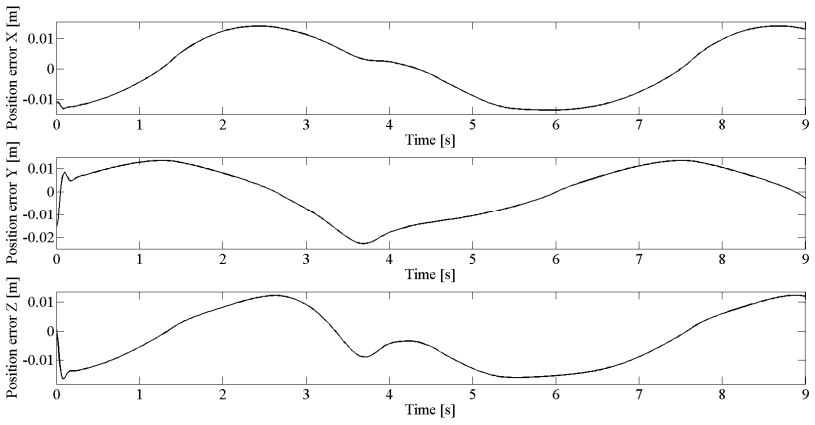

Figure7: The accuracy of achieving the position of the upper platform

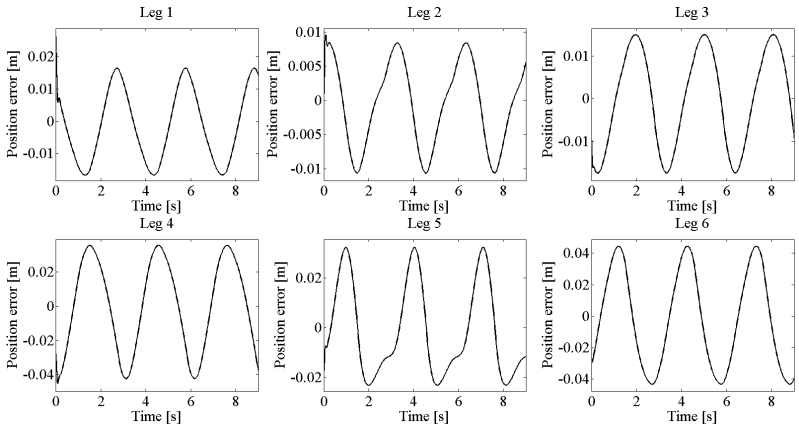

Figure8: The accuracy of achieving the positions of the pneumatically driven extensible actuators, when frequency is 2HZ

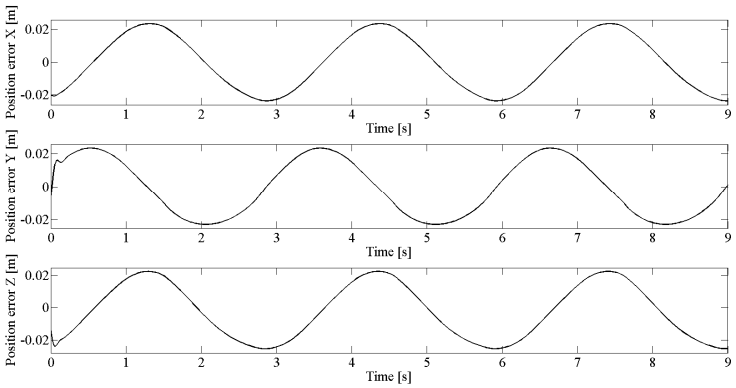

Figure9: The accuracy of achieving the position of the upper platform, when frequency is 2HZ

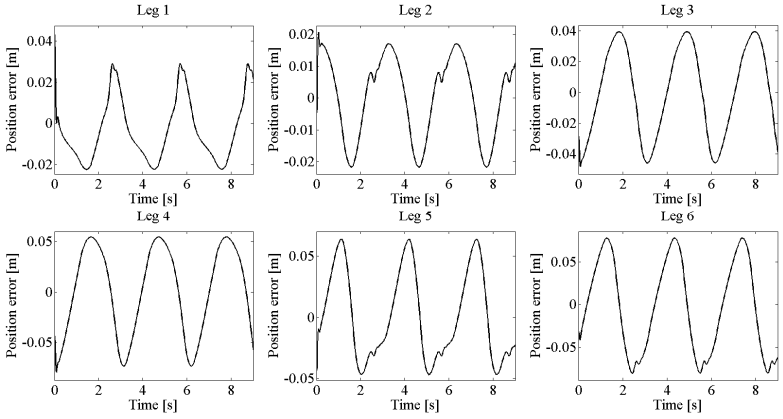

Figure10: The accuracy of achieving the positions of the pneumatically driven extensible actuators when the piston stroke is L=0.8m

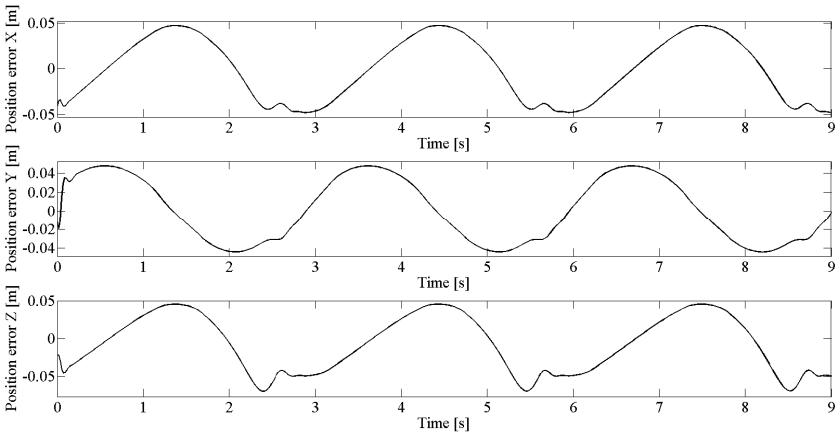

Figure11: The accuracy of achieving the position of the upper platform when the piston stroke is L=0.8m

By comparing Figures 8-9 and Figures 10-11 one can conclude that longer piston strokes affect on reduction of accuracy. This is the effect of air compressibility.

6 Conclusions

An analysis and simulation of Stewart platform manipulator behavior driven by pneumatic cylinders, applied in wood processing, are considered in this paper. Realization of the exact position of the upper moving plate presents a base for high quality woodworking. The analysis was based on the formulation of Lagrange equations of the second type, determining the Jacobian matrix for mechanical part and forming models for the pneumatic actuator. The simulation was performed using the MATLAB/Simulink software. Simulation results have shown the influence of the complexity of the desired trajectory platforms, stroke lengths and speed on the accuracy of achieving positions the platform. From simulation results one can conclude that with increasing complexity of realized trajectories, the accuracy was reduced. Further, longer piston strokes as well as higher frequency of realized trajectory also affect on reduction of accuracy.

Acknowledgements This research has been supported by the European Union through the ADRIA-HUB project from the IPA Adriatic programme.

References

[1] D. Stewart. A platform with six degrees of freedom. *Proceedings of the Institution of Mechanical Engineers, Journal of Power and Energy*, 180(15): 371–386, 1965.

[2] S. Živanović, M. Glavonjić, Z. Dimić. Configuring Of Virtual Three Axes Parallel Kinematics Milling Machine Used For Simulation And Verification Of Control And Programming, *Proceedings of the Infoteh*, Jahorina, 11: 464-469, 2012.

[3] N. Nedić, D. Pršić, D. Dubonjić. Feasibility Study of a Parallel Robot Platform With Six Degrees of Freedom in the Wood processing, The Principal Approach, (In Serbian), Faculty of Engineering Science, University of Kragujevac, ISBN: 978-86-6335-019-9, 2015.

[4] S. Küçük. Serial and Parallel Robot Manipulators – Kinematics, Dynamics, Control and Optimization. Published by *InTech*, 2012, Printed in Croatia.

[5] V. Stojanović, N. Nedić. A nature inspired parameter tuning approach to cascade control for hydraulically driven parallel robot platform. *Journal of Optimization Theory and Applications*, DOI: 10.1007/s10957-015-0706-z, 2015.

[6] H. Abdellatif, B. Heimann, Computational efficient inverse dynamics of 6-DOF fully parallel manipulators by using the Lagrangian formalism. *Mechanism and Machine Theory*, 44(1): 192-207, 2009.

[7] Y, Wang, A direct numerical solution to forward kinematics of general Stewart–Gough platforms. Robotica, 25(1): 121–128, 2007.

[8] J. Wang, D. Wang, P.R. Moore, J. Pu. Modelling study, analysis and robust servo control of pneumatic cylinder actuator systems. *IEE Proceedings, Control Theory and Applications*, 148(1):35-42, 2001.

[9] J.F. Blackburn, G. Reethof, J.L. Shearer, *Fluid Power Control*, The MIT Press Cambridge, Massachusetts, 1960.